



Published in final edited form as:

*Environ Sci Technol Lett.* 2014 February 11; 1(2): 146–151. doi:10.1021/ez400202b.

## Transport of gold nanoparticles through plasmodesmata and precipitation of gold ions in woody poplar

Guangshu Zhai<sup>1,\*</sup>, Katherine S. Walters<sup>2</sup>, David W. Peate<sup>3</sup>, Pedro J.J. Alvarez<sup>4</sup>, and Jerald L. Schnoor<sup>1</sup>

<sup>1</sup>Department of Civil and Environmental Engineering and IIHR Hydroscience and Engineering, The University of Iowa, Iowa City, IA, 52242, USA

<sup>2</sup>Central Microscopy Research Facility, The University of Iowa, Iowa City, IA, 52242, USA

<sup>3</sup>Department of Earth & Environmental Sciences, The University of Iowa, Iowa City, IA, 52242, USA

<sup>4</sup>Department of Civil and Environmental Engineering, Rice University, Houston, TX, USA

### Abstract

Poplar plants (*Populus deltoides* × *nigra*, DN-34) were used as a model to explore vegetative uptake of commercially available gold nanoparticles (AuNPs) and their subsequent translocation and transport into plant cells. AuNPs were directly taken up and translocated from hydroponic solution to poplar roots, stems and leaves. Total gold concentrations in leaves of plants treated with 15, 25 and 50 nm AuNPs at exposure concentrations of 498±50.5, 247±94.5 and 263±157 ng/mL in solutions were: 0.023±0.006, 0.0218±0.004 and 0.005±0.0003 µg/g dry weight, respectively, which accounted for 0.05, 0.10 and 0.03%, respectively, of the total gold mass added. The presence of total gold in plant tissues was measured by inductively coupled plasma mass spectrometry, while AuNPs were observed by transmission electron microscopy in plant tissues. In solution, AuNPs were distinguished from Au(III) ions by membrane separation and centrifugation. AuNPs behaved conservatively inside the plants and were not dissolved into gold ions. On the other hand, Au(III) ions were taken up and reduced into AuNPs inside whole plants. AuNPs were observed in the cytoplasm and various organelles of root and leaf cells. A distinct change in color from yellow to pink was observed as Au(III) ions were reduced and precipitated in hydroponic solution. The accumulation of AuNPs in the plasmodesma of the phloem complex in root cells clearly suggests ease of transport between cells and translocation throughout the whole plant, inferring the potential for entry and transfer in food webs.

---

\*Corresponding author Tel: +1 319 335 5647, Fax: 319 335 5660, zhai-guangshu@uiowa.edu.

#### Supporting Information Available

The method for TEM and gold determination by ICP-MS, gold concentrations in unfiltered and filtered samples of hydroponic solutions at different times and under different exposure conditions (Table S1), water volume of cumulative evapotranspiration in poplars under different conditions (Figure S1), and AuNPs in the plant (Figures S2–S11). This material is available free of charge via the Internet at <http://pubs.acs.org>.

The authors declare no competing financial interest.

## INTRODUCTION

Wide commercial and industrial applications of engineered nanoparticles (NPs) have inevitably led to their release into the environment, raising concerns about the potential for ecological effects, entry and transfer in food webs, and human exposure (1). Because of their small size and unique properties, NPs may cross cell barriers and interact with intracellular structures to cause potential cellular and genetic toxicity (2–4). However, the exact mechanisms of uptake, intercellular transport and toxicity of NPs in biota are largely unknown. Several reviews (5–8) summarized the cellular toxicity, genotoxicity, and transmission of engineered NPs in plants and animals. Gold nanoparticles (AuNPs) were one of the most frequently studied NPs because of their many commercial applications, ease of synthesis, different sizes and shapes, various coatings (9, 10, 11), chemical stability, unique optical properties (12), ease of quantitation (13), and relatively low toxicity (14–16, 17) for medical applications. Therefore, the interactions of AuNPs and biota have been of significant interest (18).

Biotransformation of gold [Au(III)] ions into AuNPs was reported in plants *in vivo* and *in vitro*. Gardea-Torresdey et al. (19) illustrated the formation of AuNPs from Au(III) ions by living plants (alfalfa), which suggested new and exciting ways to fabricate nanoparticles. In addition, 5–50 nm AuNPs were produced from Au(III) ions within *Brassica juncea* (20), and, Au(III) ions were reduced to AuNPs *in vitro* in alga and oat biomass (21, 22). Different sizes, with or without coatings, surface charges and various shapes of AuNPs had great influence on their transport in whole plants or plant cells (15, 23–25). Transfer and biomagnification of AuNPs in the food chain raise the risk of exposure of human to AuNPs. For example, detritivores took up AuNPs from soil and distributed them among various tissues (26), and trophic transfer and biomagnification of AuNPs from a primary producer to a primary consumer were characterized by mean bioaccumulation factors of 6.2, 11.6, and 9.6 for treatments with 5, 10, and 15 nm AuNPs, respectively (27). Another study showed that AuNPs could be transferred from soil media to invertebrates and then to secondary consumers (28). Because of their chemical stability and ease of detection, AuNPs have been used as the probes for the behavior of NPs within biological systems. However, most research has been performed on AuNPs in herbaceous plants (29) rather than woody plants, which have clearly defined vascular systems and multiple membranes. In this research, we investigate the uptake, translocation, transformation and transport mechanisms of commercial AuNPs and Au(III) ions into the cytoplasm of root and leaf cells in whole woody poplars.

## MATERIALS AND METHODS

### Reagents

Potassium gold (III) chloride (99.995%) was purchased from Sigma-Aldrich. Three sizes (size distribution <15%) of water soluble bare gold nanoparticles (15nm with a particle concentration of  $1.88 \times 10^{-9}$  M, 25 nm with a particle concentration of  $2.69 \times 10^{-10}$  M and 50 nm with a particle concentration of  $4.41 \times 10^{-11}$  M) were purchased from Ocean Nano Tech, LLC (Springdale, AR). The deionized water ( $18.3 \text{M}\Omega$ ) was from an ultrapure water system (Barnstead International, Dubuque, IA, USA). The reagents (nitric acid, hydrochloric acid

and hydrogen peroxide) in inductively coupled plasma mass spectrometry (ICP-MS) methods were trace-metal reagents. All other chemicals and reagents used in this experiment were of analytical reagent grade or better.

### Poplar growth and treatment

Six-inch cuttings (Segal Ranch, WA) of hybrid poplar plants (*Populus deltoides* × *nigra*, DN34) were used in exposure experiments after the plants had grown for 25 days in ½-strength Hoagland solution. The preparation of cuttings, their growth, and exposure method were similar to those described previously (30). In brief, healthy vigorously growing poplar plants were selected for the AuNPs and Au(III) ion exposure experiments. The exposure reactors consisted of 250-mL glass conical flasks with a PTFE-faced septum sampling port. All the exposure reactors and deionized water for Hoagland nutrient solution were autoclaved prior to being used. Then, different concentrations of AuNPs and Au(III) ions were added to 200 mL of DI water in the reactors. The 3 mL of 15 nm, 25 nm or 50 nm AuNP standard solution was added in each reactor except for the blank poplar controls without AuNPs. As shown in Table S1, the approximate initial exposure concentrations were measured as 498±50.5, 247±94.5 and 263±157 ng/mL for the 15 nm, 25, and 50 nm exposures, respectively. The final exposure concentration of Au(III) ions into each reactor was 5.0, 10.0 and 20.0 mg/L, respectively, except for the blank poplar control without Au(III) ions. Blank plant controls were three whole poplar plants without AuNPs and Au(III) ions; whole poplar plants [three whole, growing, intact poplar plants with AuNPs and Au(III) ions] were used to test the transport and biotransformation in poplar plants. All exposure reactors were wrapped with aluminum foil and kept at 23±1°C. The photoperiod was set to 16 h per day under fluorescent lighting with a light intensity between 120 and 180 μmol m<sup>-2</sup> s<sup>-1</sup> and DI water saturated with oxygen was injected into the reactors twice per day to compensate for the evapotranspiration loss, which was determined by monitoring the weight loss of the reactors. Cumulative evapotranspiration for each poplar plants was the sum of the evapotranspiration during the 6 day exposure.

### Method for Transmission Electron Microscopy (TEM) and gold determination by ICP-MS

Methods of AuNPs for TEM and determination of gold concentrations by ICP-MS in leaf and roots are shown in the Supporting Information in detail.

## RESULTS AND DISCUSSION

The toxicity of AuNPs and Au(III) ions to poplars was inferred by measuring the rate and extent of evapotranspiration. Decreased rates of evapotranspiration are a reliable indicator of decreased biomass growth and toxicity to the plant (31). Poplars exposed to 15, 25 and 50 nm AuNPs had evapotranspiration rates statistically equivalent to those of the controls, suggesting that AuNPs did not have any adverse effects on poplar at the experimental concentrations (Figure S1A of the Supporting Information). However, water cumulative evapotranspiration volumes decreased sharply for poplars treated with 5 to 20 mg/L (25.4 μM to 101.5 μM) of Au(III) ions (Figure S1B of the Supporting Information), which suggested that Au(III) ions exerted toxicity to poplars at high concentrations. When exposed hydroponically to Au(III) concentrations of 20 mg/L, the poplars experienced a great

decrease in the level of cumulative evapotranspiration compared to that upon exposure at 10 mg/L. However, the plants survived the 6 day exposure even at 20 mg/L Au(III) ions. A decreased rate of evapotranspiration at 20 mg/L resulted in reduced gold concentrations in leaves as measured by ICP-MS. Thus, more gold actually accumulated in the leaves of plants exposed to 10 mg/L Au(III) because there was less inhibition (greater evapotranspiration).

Gold concentrations were measured in filtered and unfiltered samples by ICP-MS to assess transformation between AuNPs and Au(III) ions from the hydroponic solutions (Figure 1A–C and Table S1 of the Supporting Information). Centrifugal filtration was used to operationally define Au(III) ion concentrations as those that pass the centrifugal filter (Amicon Ultra-4 3K centrifugal filter devices). First, we noticed that AuNPs were quickly removed from the solution (Figure 1A) by poplar uptake, and gold was not detected in the corresponding filtered samples (Table S1 of the Supporting Information), suggesting that AuNPs did not oxidize and release Au(III) ions. In separate experiments, Au(III) ions were also quickly taken up by poplars from solution (Figure 1B). A comparison of total gold concentrations in the filtered and unfiltered samples (Figure 1B, C) infers that >90% of Au(III) ions were transformed into AuNPs in the hydroponic solution. This phenomenon was confirmed by TEM images (Figure 2) and by observations of the change in color from yellow to pink [a redox reaction from Au(III) to Au(0)]. A large number of AuNPs were produced from Au(III) ions (20 mg/L) within 2 days in this solution in the presence of poplars. These AuNPs had relatively uniform sizes, ranging from 20 to 40 nm. AuNPs were also observed on the surface of bacteria in the solution, similar to CdNPs on the surface of bacteria found previously (32). Similar phenomena were observed in the hydroponic solutions of poplars exposed to 5 and 10 mg/L Au(III) ions. Because no AuNPs were formed in sterile medium without poplars, we postulate that this transformation is due to the exudates from plant roots, including mucilage, enzymes, sugars, phenolics, and amino acids (33), which could reduce Au(III) ions to elemental AuNPs. Therefore, Au(III) ions can be transformed into AuNPs; However, the reaction is not reversible, and AuNPs were not transformed into Au(III) ions in the hydroponic solution with poplars.

Total gold concentrations in the leaves of poplar plants exposed for 6 days were analyzed to evaluate the translocation of AuNPs and Au(III) ions from solutions (Figure 1D). Total gold concentrations in leaves exposed to AuNPs were much lower than those in leaves exposed to Au(III) ions. Total gold concentrations in leaves of plants treated with 15, 25 and 50 nm AuNPs were  $0.023 \pm 0.006$ ,  $0.0218 \pm 0.004$  and  $0.005 \pm 0.0003$   $\mu\text{g/g}$  of dry weight, respectively, which accounted for 0.05, 0.10 and 0.03%, respectively, of the total gold mass added. Higher total gold concentrations were found in leaves treated with 5, 10 and 20 mg/L Au(III) ions, reaching  $2.05 \pm 0.96$ ,  $15.9 \pm 8.87$  and  $1.55 \pm 0.41$   $\mu\text{g/g}$  of dry weight, which accounted for 0.78, 2.59 and 0.04%, respectively, of the total gold mass added. Higher total gold concentrations accumulated in the leaves of trees exposed hydroponically to 10 mg/L Au(III) ions than in the leaves treated with 20 mg/L Au(III) ions because of an increased toxicity and decreased rate of evapotranspiration (inhibition) exerted by the latter (Figure S1 of the Supporting Information).

TEM images proved the presence and distribution of AuNPs in roots and leaves of poplars exposed to AuNPs and Au(III) ions. AuNPs adhered to the external surface of the primary roots and secondary roots, which was visible to the naked eye by the pink coloration of white roots. In addition, AuNPs were found in the specific cells of roots and leaves of plants exposed to 15, 25 and 50 nm AuNPs (Figures 3 and Figures S2–S4 of the Supporting Information), such as the phloem complex (including companion cells and sieve tube members) and xylem cells of the roots. The specific sites where AuNPs accumulated inside the root cells were the cytoplasm, cell wall, plastid, mitochondria, and especially the plasmodesmata. In the leaves, AuNPs were observed mainly inside the xylem cells and on xylem cell walls, indicating translocation from roots through xylem. The size distribution of the AuNPs appears to be somewhat modified (less uniform) during uptake and transport with the exception of 50 nm AuNPs, which maintained their diameter but were surrounded by some unknown substances in leaf xylem cells (Figure S4 of the Supporting Information). In addition, AuNPs were more abundant in the roots than in the leaves because the roots directly contacted AuNPs in the solution, but only a small fraction of the AuNPs added to the solution were translocated to the leaves.

The sites and sizes of AuNPs in the roots and leaves exposed to Au(III) ions varied greatly (Figures 4 and Figures S4–S12 of the Supporting Information), ranging from extremely small AuNPs (<1 nm) to large AuNPs (aggregated particles). In addition, AuNPs were distributed throughout the plant. Small-diameter AuNPs precipitated around the cell membranes and inside the cells (Figures 3–4 and Figures S7–S9 of the Supporting Information). AuNPs were observed in cell membranes, cytoplasm, mitochondria, chloroplast and other unidentified organelles. Furthermore, AuNPs in poplar roots showed a difference from those in poplar leaves.

Although NPs, including AuNPs, have been previously observed in plants, their mechanism of uptake and transport into the plant cells is not well understood. Generally, transport of NPs into plant cells is hindered by the plant cell wall, which has pore sizes ranging from 2 to 20 nm and represents a barrier (along with the cell membrane) for cellular uptake. Therefore, it is difficult for the larger NPs to penetrate.

Potential modes of uptake of NPs by plant cells have been previously summarized (6). NPs may be bound to carrier proteins or organic chemicals and enter plant cells through aquaporins, or ion channels, or by endocytosis; NPs may be transported apoplastically or symplastically inside the cells, and NPs can be transported from one cell to another through plasmodesmata, which consist of three main layers, including the plasma membrane, the desmotubule and the cytoplasmic sleeve. Furthermore, because of virtually no cytoplasm in sieve tube members, the desmotubule provides a continuum between the parietal endoplasmic reticulum (ER) of the sieve tube member and the normal, cortical ER of the companion cell. Therefore, NPs may pass through plasmodesmata between sieve tube members and companion cells via the ER-mediated mode of the transport pathway (34). In this study, plasmodesmata with AuNPs were found in the discontinuous channels around the cell wall of companion cells and sieve tube members, which suggests an ER-mediated transport pathway. TEM images revealed the plasmodesmata as the primary transport mechanism of AuNPs in whole woody poplar plants exposed to AuNPs (15, 25 and 50 nm).

AuNPs penetrated the epidermal and root hair cell walls and root caps and entered the poplar roots. They were subsequently translocated to leaves via xylem and phloem (Figure 3 and Figures S2–S4 of the Supporting Information). Figure 3 illustrates this transport mechanism for AuNPs based on the location of AuNPs in the phloem complex. AuNPs accumulated in the plasmodesmata, revealing this transport mechanism as a rate determining step. AuNPs moved inside the roots via sieve tube members and xylems. Sieve tube members are a specialized type of elongated cell in the phloem tissue, and the ends of these cells are connected with other sieve tube members to constitute the sieve tube, which transports nutrients throughout the plant. Because sieve tube members are living cells (and lack a cell nucleus, ribosomes, or vacuoles at maturity), each sieve tube member is normally associated with one or more nucleate companion cells to provide proteins, ATP, and signaling molecules by plasmodesmata (the channels between the cells). We postulate that AuNPs entered into the sieve tube members and xylem of roots and then translocated to leaves along the sieve tubes and xylems. AuNPs in sieve tubes were transported to companion cells via plasmodesmata on the cell wall, where AuNPs aggregated because of the narrowing of these channels. This would explain the observed dark blocks at regular intervals around the cell walls (Figure 3A, B).

The aggregation of gold nanoparticles in the plasmodesmata could influence the transport of nutrients and other materials from companion cells, which may produce the toxic effect observed on poplars from exposure to Au(III) ions. Also AuNPs were found in the plastids and p-proteins in the sieve tube members. A small number of AuNPs were found inside the leaves and mainly existed in the xylem (Figure 3D, E), suggesting that AuNPs also followed the transmission route of water and nutrients through the xylem to the leaves.

## Supplementary Material

Refer to Web version on PubMed Central for supplementary material.

## Acknowledgments

We thank N. M. Shahmansouri for help with sample preparation. This research was funded by the National Science Foundation (CMMI-1057906) and a subcontract between Rice University and the University of Iowa, W.M. Keck Phytotechnologies Laboratory. The establishment of the ICP-MS laboratory (EAR-0821615) was supported by the National Science Foundation. In addition, this work was supported by the Iowa Superfund Research Program (isrp) National Institute of Environmental Health Science, Grant P42ES013661.

## REFERENCES

1. Gottshalk F, Sonderer T, Scholz RW, Nowack B. Modeled environmental concentrations of engineered nanomaterials (TiO<sub>2</sub>, ZnO, Ag, CNT, Fullerenes) for different regions. *Environ. Sci. Technol.* 2009; 43:9216–9222. [PubMed: 20000512]
2. Zhang L, Gu F, Chan J, Wang A, Langer RS, Farokhzad OC. Nanoparticles in medicine: therapeutic applications and developments. *Clin. Pharmacol. Ther.* 2008; 83:761–769. [PubMed: 17957183]
3. Navarro E, Baun A, Behra R, Hartmann NB, Filser J, Miao AJ, Quigg A, Santschi PH, Sigg L. Environmental behavior and ecotoxicity of engineered nanoparticles to algae, plants, and fungi. *Ecotoxicology.* 2008; 17:372–386. [PubMed: 18461442]
4. Handy RD, Owen R, Valsami-Jones E. The ecotoxicology of nanoparticles and nanomaterials: Current status, knowledge gaps, challenges, and future needs. *Ecotoxicology.* 2008; 17:315–325. [PubMed: 18408994]

5. Remedios C, Rosario F, Bastos V. Environmental nanoparticles interactions with plants: Morphological, physiological, and genotoxic aspects. *J. Bot.* 2012
6. Rico CM, Majumdar S, Duarte-Gardea M, Peralta-Videa JR, Gardea-Torresdey JL. Interaction of nanoparticles with edible plants and their possible implications in the food chain. *J. Agric. Food Chem.* 2011; 59:3485–3498. [PubMed: 21405020]
7. Khlebtsov N, Dykman L. Biodistribution and toxicity of engineered gold nanoparticles: A review of in vitro and in vivo studies. *Chem. Soc. Rev.* 2011; 40:1647–1671. [PubMed: 21082078]
8. Ma X, Geiser-Lee J, Deng Y, Kolmakov A. Interactions between engineered nanoparticles (ENPs) and plants: Phytotoxicity, uptake and accumulation. *Sci. Total Environ.* 2010; 408:3053–3061. [PubMed: 20435342]
9. Brust M, Kiely CJ. Some recent advances in nanostructure preparation from gold and silver particles: a short topical review. *Colloids Surf., A.* 2002; 202:175–186.
10. Grzelczak M, Perez-Juste J, Mulvaney P, Liz-Marzan LM. Shape control in gold nanoparticle synthesis. *Chem. Soc. Rev.* 2008; 37:1783–1791. [PubMed: 18762828]
11. Su YH, Tu SL, Tseng SW, Chang YC, Chang SH, Zhang WM. Influence of surface plasmon resonance on the emission intermittency of photoluminescence from gold nano-sea-urchins. *Nanoscale.* 2010; 2:2639–2646. [PubMed: 20967388]
12. Raschke G, Kowarik S, Franzl T, Solnichen C, Klar TA, Feldmann J, Nichtl A, Kuirzinger K. Biomolecular recognition based on single gold nanoparticle light scattering. *Nano Lett.* 2003; 3:935–938.
13. Yu L, Andriola A. Quantitative gold nanoparticle analysis methods: A review. *Talanta.* 2010; 82:869–875. [PubMed: 20678639]
14. Goodman CM, McCusker CD, Yilmaz T, Rotello VM. Toxicity of gold nanoparticles functionalized with cationic and anionic side chains. *Bioconjugate Chem.* 2004; 15:897–900.
15. Chen Y, Hung Y, Liau I, Huang GS. Assessment of the in vivo toxicity of gold nanoparticles. *Nanoscale Res. Lett.* 2009; 4:858–864. [PubMed: 20596373]
16. Uboldi C, Bonacchi D, Lorenzi G, Hermanns MI, Pohl C, Baldi G, Unger RE, Kirkpatrick CJ. Gold nanoparticles induce cytotoxicity in the alveolar type-II cell lines A549 and NCIH441. *Part. Fibre Toxicol.* 2009; 6:18. [PubMed: 19545423]
17. Sabo-Attwood T, Unrine JM, Stone JW, Murphy CJ, Ghoshroy S, Blom D, Bertsch PM, Newman LA. Uptake, distribution and toxicity of gold nanoparticles in tobacco (*Nicotiana xanthi*) seedlings. *Nanotoxicology.* 2012; 6:353–360. [PubMed: 21574812]
18. Chithrani BD, Ghazani AA, Chan WCW. Determining the size and shape dependence of gold nanoparticle uptake into mammalian cells. *Nano Lett.* 2006; 6:662–668. [PubMed: 16608261]
19. Gardea-Torresdey JL, Parsons JG, Gomez E, Peralta-Videa J, Troiani HE, Santiago P, Yacaman MJ. Formation and growth of Au nanoparticles inside live alfalfa plants. *Nano Lett.* 2002; 2:397–401.
20. Marshall AT, Haverkamp RG, Davies CE, Parsons JG, Gardea-Torresdey JL, van Agterveld D. Accumulation of gold nanoparticles in *Brassic juncea*. *Int. J. Phytorem.* 2007; 9:197–206.
21. Greene B, Hosea M, McPherson R, Henzl M, Alexander MD, Darnall DW. Interaction of gold (I) and gold (III) complexes with algal biomass. *Environ. Sci. Technol.* 1986; 20:627–632. [PubMed: 19994962]
22. Armendariz V, Herrera I, Peralta-Videa JR, Jose-Yacaman M, Troiani H, Santiago P, Gardea-Torresdey JL. Size controlled gold nanoparticle formation by *Avena sativa* biomass: use of plants in nanobiotechnology. *J. Nanopart. Res.* 2004; 6:377–382.
23. Hawthorne J, Musante C, Sinha SK, White JC. Accumulation and phytotoxicity of engineered nanoparticles to *cucurbita pepo*. *Int. J. Phytorem.* 2012; 14:429–442.
24. Judy JD, Unrine JM, Rao W, Wirick S, Bertsch PM. Bioavailability of gold nanomaterials to plants: Importance of particle size and surface coating. *Environ. Sci. Technol.* 2012; 46:8467–8474. [PubMed: 22784043]
25. Zhu ZJ, Wang H, Yan B, Zheng H, Jiang Y, Miranda OR, Rotello VM, Xing B, Vachet RW. Effect of surface charge on the uptake and distribution of gold nanoparticles in four plant species. *Environ. Sci. Technol.* 2012; 46:12391–12398. [PubMed: 23102049]

26. Unrine JM, Hunyadi SE, Tsyusko OV, Rao W, Shoultz-Wilson WA, Bertsch PM. Evidence for bioavailability of Au nanoparticles from soil and biodistribution within earthworms (*Eisenia fetida*). *Environ. Sci. Technol.* 2010; 44:8308–8313. [PubMed: 20879765]
27. Judy JD, Unrine JM, Bertsch PM. Evidence for biomagnification of gold nanoparticles within a terrestrial food chain. *Environ. Sci. Technol.* 2011; 45:776–781. [PubMed: 21128683]
28. Unrine JM, Shoultz-Wilson WA, Zhurbich O, Bertsch PM, Tsyusko OV. Trophic transfer of Au nanoparticles from soil along a simulated terrestrial food chain. *Environ. Sci. Technol.* 2012; 46:9753–9760. [PubMed: 22897478]
29. Miralles P, Church TL, Harris AT. Toxicity, uptake, and translocation of engineered nanomaterials in vascular plants. *Environ. Sci. Technol.* 2012; 46:9224–9239. [PubMed: 22892035]
30. Zhai G, Lehmler H-J, Schnoor JL. Hydroxylated metabolites of 4-monochlorobiphenyl and its metabolic pathway in whole poplar plants. *Environ. Sci. Technol.* 2010; 44:3901–3907. [PubMed: 20402517]
31. Dietz AC, Schnoor JL. Phytotoxicity of chlorinated aliphatics to hybrid poplar (*Populus deltoides* × *nigra* DN34). *Environ. Toxicol. Chem.* 2001; 20:389–393. [PubMed: 11351440]
32. Yang Y, Mathieu JM, Chattopadhyay S, Miller JT, Wu T, Shibata T, Guo W, Alvarez PJJ. Defense mechanisms of *Pseudomonas aeruginosa* PAO1 against quantum dots and their released heavy metals. *ACS Nano.* 2012; 6:6091–6098. [PubMed: 22632375]
33. Marschner, H. Mineral Nutrition of Higher Plants. San Diego: Academic Press; 1995.
34. Roberts AG, Oparka KJ. Plasmodesmata and the control of symplastic transport. *Plant, Cell Environ.* 2003; 26:103–124.



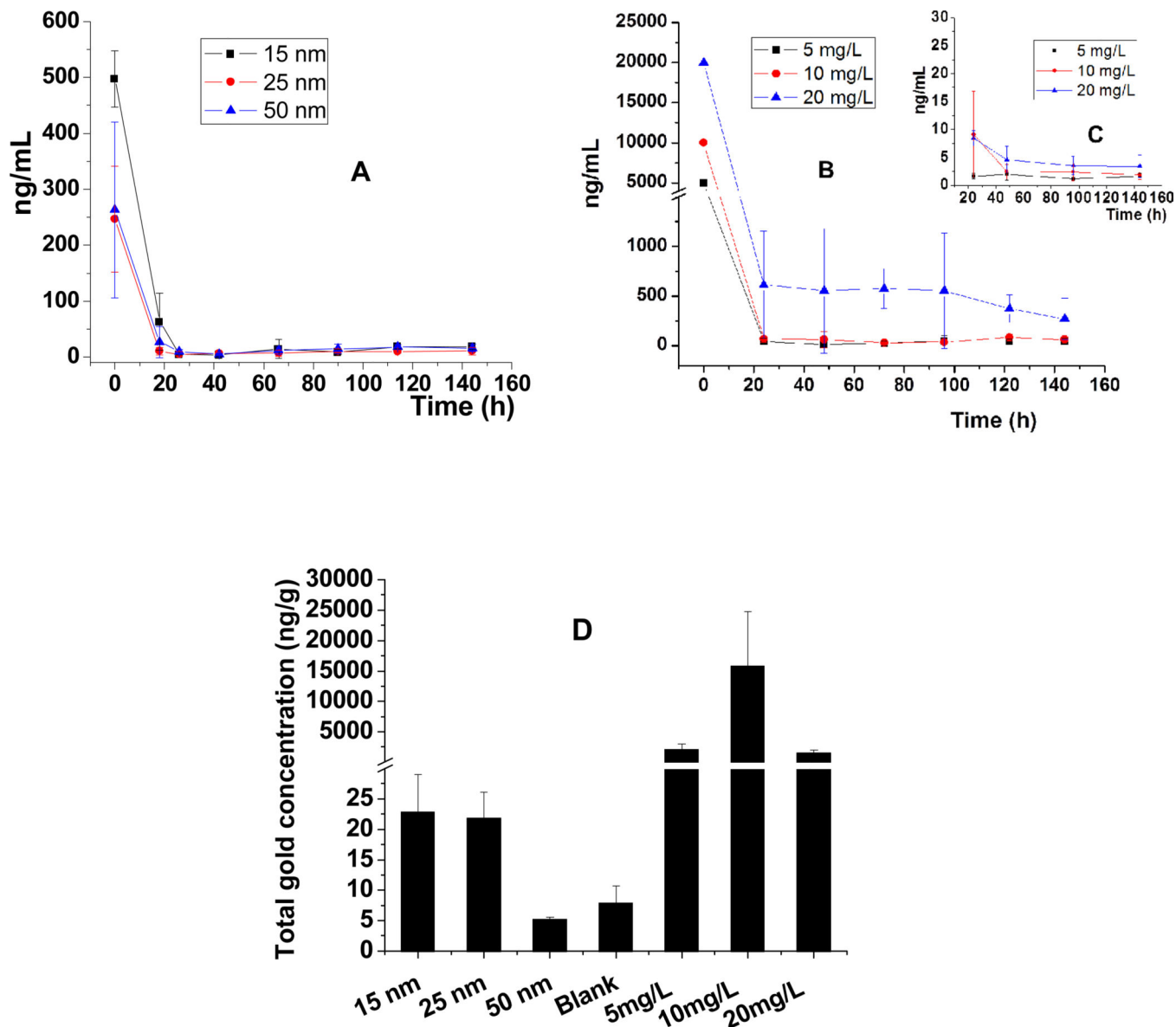


**Fig. 1. Total gold concentrations over time in hydroponic solutions of flasks with hybrid poplar plants exposed to AuNPs and gold ions**

(A) Total gold concentrations in the solution with AuNPs added at time zero. (B) Total gold concentrations in the solution with Au(III) ions introduced at time zero. (C) Au(III) ion concentrations (filtered samples) from a solution in the experiment used to create panel B. (D) Total gold concentrations in leaves (nanograms per gram of dry weight) exposed to AuNPs (15, 25, and 50 nm) and Au(III) ions (5, 10, and 20 mg/L).

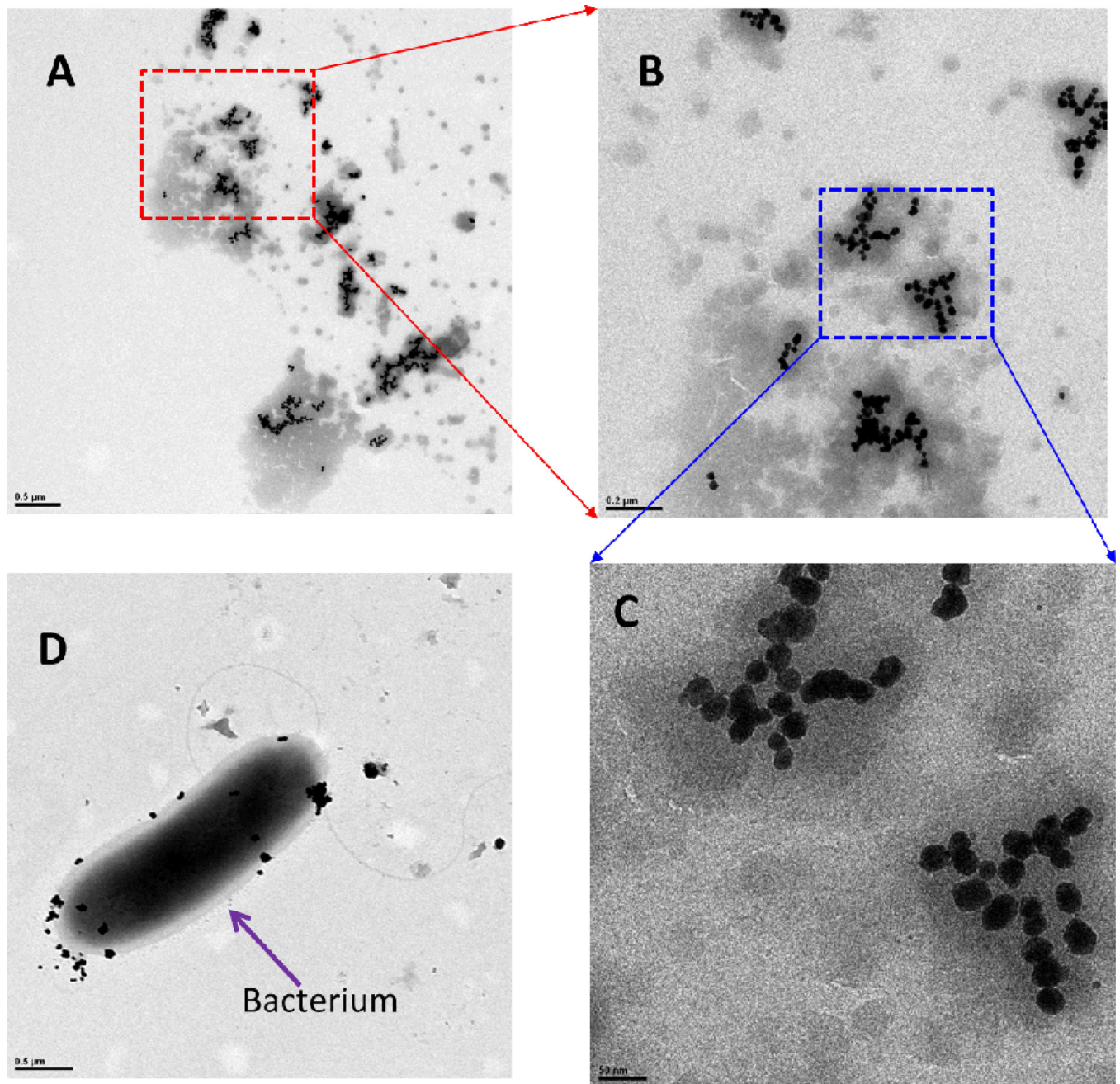


**Fig. 2.** TEM images of AuNPs in the hydroponic solution where poplars were exposed to 20 mg/L of Au(III) ion for 2 days

(A) AuNPs in the solution, (B) magnified A, (C) magnified B, and (D) bacterium with AuNPs.

Scale bars of (A) 0.5 μm, (B) 0.2 μm, (C) 50 nm, and (D) 0.5 μm.

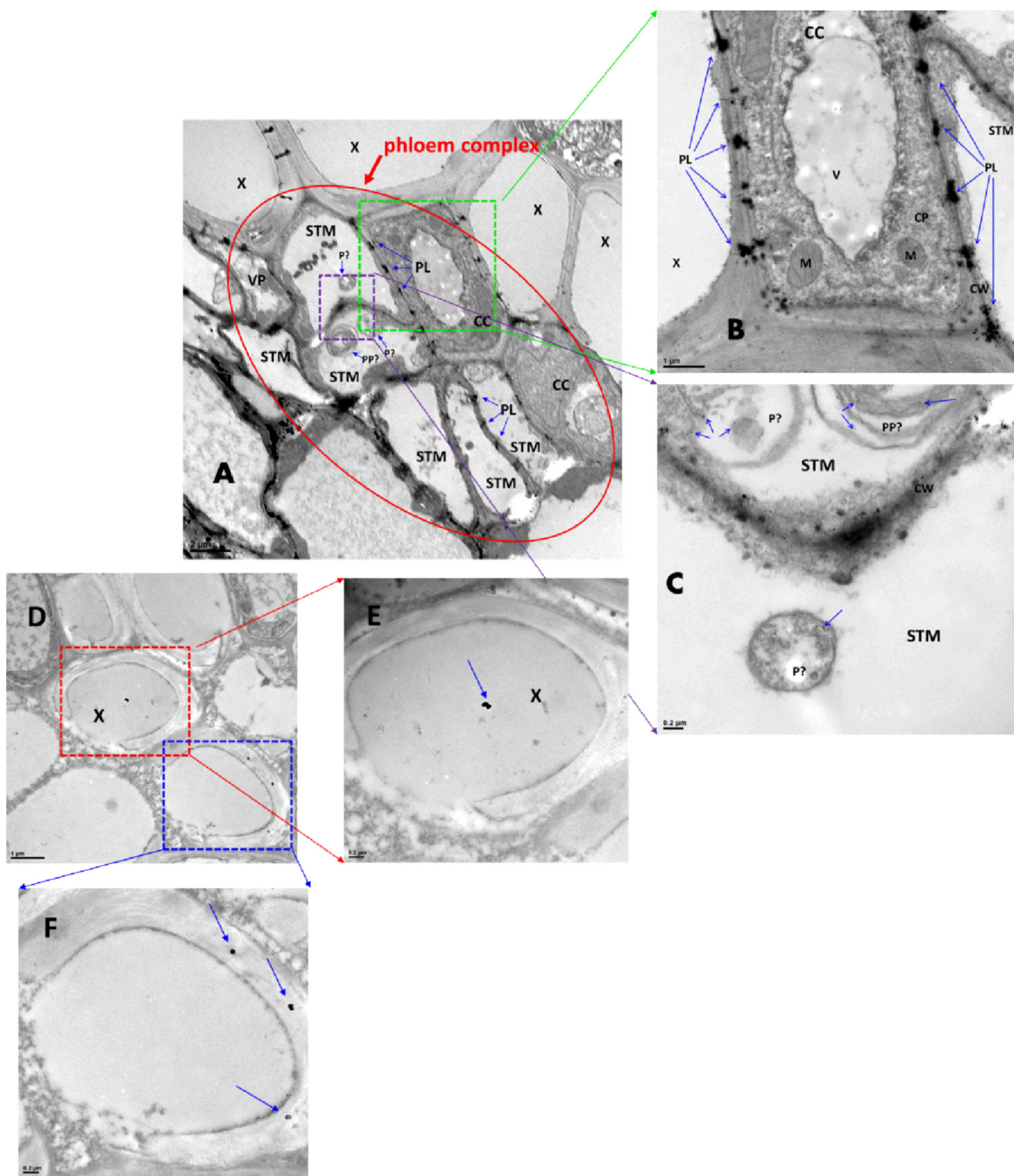


**Fig. 3.** AuNPs in roots (A–C) and leaves (D–F) of poplars exposed to 15 nm AuNPs on day 6  
 Abbreviation: CC, companion cell; CP, cytoplasm; CW, cell wall; M, mitochondria; P, plastid; PL, plasmodesmata; PP, P-protein; STM, sieve tube member; V, vacuole; VP, vascular parenchyma cell; X, xylem;  
 Scale bars of (A) 2  $\mu\text{m}$ , (B) 1  $\mu\text{m}$ , (C) 0.2  $\mu\text{m}$ , (D) 1  $\mu\text{m}$ , (E) 0.2  $\mu\text{m}$ , and (F) 0.2  $\mu\text{m}$ .

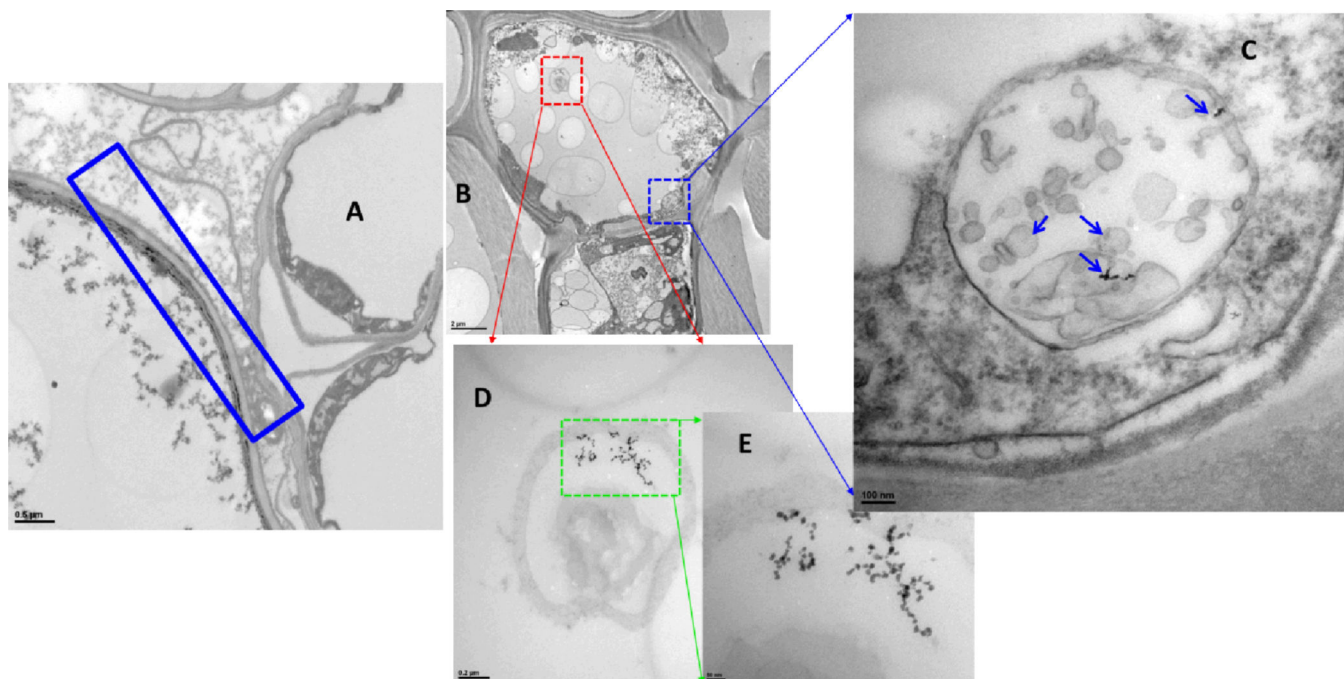


**Fig. 4.** Precipitation of AuNPs in the roots (A) and leaves (B–E) of poplars exposed to 10 mg/L Au(III) ions on day 6  
Scale bars of (A) 0.5  $\mu\text{m}$ , (B) 2  $\mu\text{m}$ , (C) 100 nm, (D) 0.2  $\mu\text{m}$ , and (E) 50 nm.